

Ethynyl-Capped Hyperbranched Conjugated Polytriazole: Click Polymerization, Clickable Modification, and Aggregation-Enhanced Emission

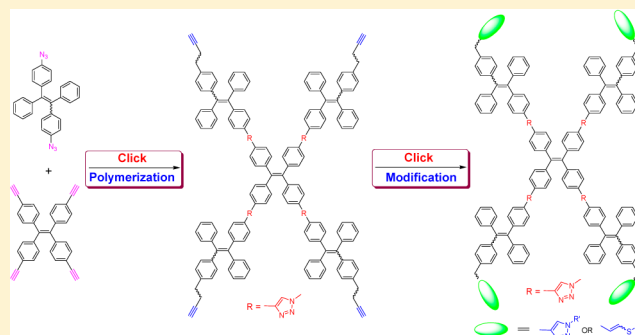
Jian Wang,[†] Ju Mei,[†] Engui Zhao,[‡] Zhegang Song,[‡] Anjun Qin,^{*,†} Jing Zhi Sun,^{*,†} and Ben Zhong Tang^{*,†,‡}

[†]MOE Key Laboratory of Macromolecular Synthesis and Functionalization, Department of Polymer Science and Engineering, Zhejiang University, Hangzhou 310027, China

[‡]Department of Chemistry, Institute for Advanced Study, Institute of Molecular Functional Materials, State Key Laboratory of Molecular Neuroscience, and Division of Biomedical Engineering, The Hong Kong University of Science & Technology, Clear Water Bay, Kowloon, Hong Kong, China

Supporting Information

ABSTRACT: Cu(I)-catalyzed azide–alkyne click polymerization, developed based on the click reaction, has become a powerful tool for the construction of functional polytriazoles with linear and hyperbranched structures. This method has, however, rarely been used for the preparation of functional hyperbranched conjugated polytriazoles (*hb*-CPTA). In this paper, soluble ethynyl-capped *hb*-CPTA with weight-averaged molecular weight of 39 500 was synthesized in high yield (84.4%) by the Cu(I)-catalyzed azide–alkyne click polymerization of tetraphenylethene containing diazide [1,2-bis(4-azidophenyl)-1,2-diphenylethene] and tetrayne [1,1,2,2-tetrakis(4-ethynylphenyl)ethane] in equal concentration. By taking advantage of the ethynyl groups on its periphery, the polymer could be efficiently postfunctionalized by azide–alkyne and thiol–yne click reactions. The polymers are thermally stable and loss 5% of their weights at temperatures higher than 340.0 °C. *hb*-CPTA also possesses high char yield (74.8%) at 800 °C. The polymers feature the unique characteristics of aggregation-enhanced emission. Furthermore, the PL intensities of the *hb*-CPTA and thiol–yne postfunctionalized polytriazoles increase linearly with water fraction in THF/water mixtures. Thanks to their rigid structures, the polymers could be fabricated into unimolecular nanoparticles with sizes of ca. 100 nm. Thus, this paper provides a powerful method to synthesize soluble ethynyl-capped hyperbranched polymers, which could be a useful platform for preparation of versatile functional polymers via postreactions.



INTRODUCTION

Cu(I)-catalyzed azide–alkyne click reaction, reported independently by Sharpless and Meldal and co-workers in 2002,¹ has become a versatile and powerful synthetic tool with applicability in diverse areas including bioconjugate synthesis and surface modification, etc.² It enjoys the advantages of high efficiency, regioselectivity, mild reaction conditions, atom economy, and tolerance to functional groups and has great potential to be developed into a powerful polymerization method. It does have been utilized in polymers science but with emphasis on the postfunctionalization of preformed polymers.³ We and others have endeavored to develop the click reaction into a click polymerization. Functional linear polytriazoles and dendrimers have been successfully prepared;^{4,5} the hyperbranched polymers were, however, rarely reported by this powerful tool.

Although structurally imperfect, a hyperbranched polymer can be facilely synthesized via a single-step reaction by a one-

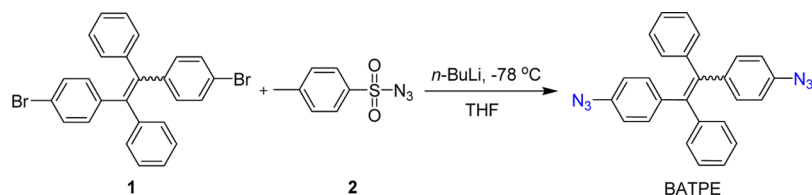
pot procedure, making them particularly desirable candidates for bulk-material and large-scale applications in diverse areas, such as nanoscale catalysis, drug delivery, and adhesive coatings.⁶ With persistent efforts of the scientists, various polymerization methods, such as polycondensation, polycyclotrimerization, and polycoupling reactions, have been developed and functional hyperbranched polymers have been obtained.⁷ Besides the harsh reaction conditions required in these polymerizations, the resultant hyperbranched polymers bearing emissive units, such as triphenylamine, fluorene, and carbazole in their branches or on their periphery, generally suffer from an upsetting “aggregation-caused quenching” (ACQ) effect; that is, their intense emission in dilute solution is weakened or even annihilated in condensed phases resulting from energy transfer

Received: August 12, 2012

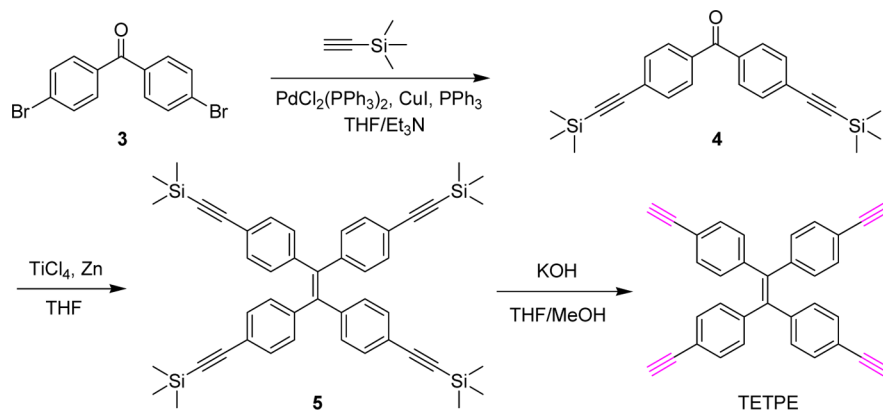
Revised: September 12, 2012

Published: September 24, 2012

Scheme 1. Synthetic Route to Diazide BATPE



Scheme 2. Synthetic Route to Tetrayne TETPE



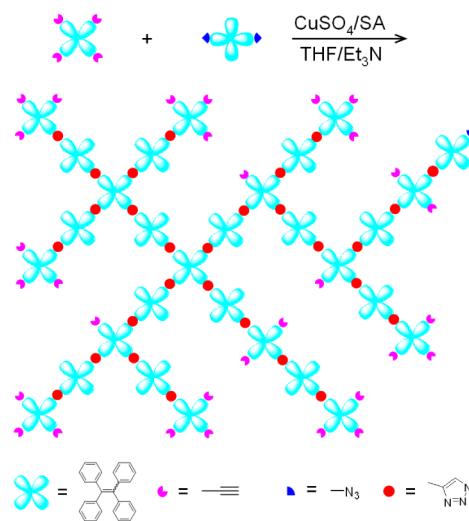
and the formation of excimers and exciplexes.⁸ This undesirable ACQ effect greatly hinders their further broad applications in optoelectronic devices, fluorescent chemosensors, and bioprobes since the light-emitting hyperbranched polymers are always applied in solid or aggregate states.⁹ Thus, preparation of hyperbranched polymers whose emission intensity could be enhanced instead of being decreased in the solid or aggregate states by efficient polymerization method with mild reaction conditions is highly desirable.

We have recently discovered an abnormal photophysical phenomenon of “aggregation-induced emission” (AIE), which is exactly opposite to the ACQ effect.¹⁰ A series of propeller-shaped luminogens, such as silole and tetraphenylethene (TPE), are nonemissive when molecularly dissolved but induced to emit efficiently by aggregate formation. Restriction of intramolecular rotation (RIR) of the multiple phenyl rotors in the aggregates has been proven experimentally and theoretically as the main cause for the AIE effect.¹¹ With the novel AIE effect, researchers can buoyantly take advantage of aggregate formation, instead of painfully fighting against the nature process of molecule aggregation. Thanks to their unique AIE characteristics, the molecules have been found to serve as chemosensors, bioprobes, stimuli-responsive nanomaterials, and active layers of efficient organic light-emitting diodes.¹²

During the course of developing click chemistry into a powerful click polymerization, we have succeeded in preparation of linear and hyperbranched polytriazoles with advanced properties, including AIE or aggregation-enhanced emission (AEE) characteristics.¹³ However, the AIE or AEE-active conjugated hyperbranched polytriazoles, which are expected to perform better than the nonconjugated ones in fluorescent sensor and bioimaging applications as well as organic light-emitting diodes, etc.,¹⁴ are rarely reported.

In this paper, we report the preparation and postfunctionalization of the first example of soluble AEE-active hyperbranched conjugated polytriazole (*hb*-CPTA) by the facile and efficient Cu(I)-catalyzed click polymerization of diazide BATPE

(A_2) and tetrayne TETPE (B_4) (Schemes 1 and 2). Through adjusting the monomer stoichiometry, ethynyl-capped 1,4-regioregular *hb*-CPTA with satisfactory molecular weight (M_w : 39 500) was obtained in high yield (84.4%) (Scheme 3), which

Scheme 3. Schematic Illustration of Synthetic Route to Ethynyl-Capped Hyperbranched Conjugated Polytriazole (*hb*-CPTA) (SA = Sodium Ascorbate)

enables us to postmodify it by azide–alkyne and thiol–yne click reactions. Photoluminescence measurements showed that *hb*-CPTA and its postmodified products are AEE active with high solid state quantum yields up to 93.5%.

RESULTS AND DISCUSSION

Monomer Preparation. Different from our previous $\text{A}_2 + \text{B}_3$ strategy, we adopted an $\text{A}_2 + \text{B}_4$ monomer pairs to construct *hb*-CPTA by click polymerization.¹⁵ TPE cored 1,2-bis(4-azidophenyl)-1,2-diphenylethene (A_2 , BATPE) and 1,1,2,2-

tetrakis(4-ethynylphenyl)ethane (B_4 , TETPE) were thus designed and synthesized. The reaction of 1,2-bis(4-bromophenyl)-1,2-diphenylethane (**1**) and tosylazide (**2**) in the presence of *n*-BuLi readily furnish BATPE in satisfactory yield (Scheme 1), whereas TETPE was prepared with following routes: McMurry homocoupling of 4,4'-bis(trimethylsilyl)-benzophenone (**4**), synthesized by Sonogashira reaction of 4,4'-dibromobenzophenone (**3**) and (trimethylsilyl)acetylene, in the presence of $TiCl_4$, and zinc powder in tetrahydrofuran (THF) afforded TPE derivative **5**. Desilylation of **5** by KOH in methanol and THF mixture furnished TETPE as pale yellow solid (Scheme 2). The monomer structures were confirmed by spectroscopic analyses (see Supporting Information for detailed characterization data; their high-resolution spectra are shown in Figures S1 and S2). The 1H NMR spectrum of BATPE (inset of Figure 3B) indicated that it is composed of almost equivalent *E/Z*-isomers. We have tried to separate them to obtain pure *E*- or *Z*-BATPE but failed probably due to their high similarities in molecular structures and polarities. Thanks to the symmetry of TETPE, needle-shaped single crystal suitable for X-ray structure analysis could be easily grown from its chloroform solution by slow evaporation of solvent (Figure 1 and Table S1), which provided a direct proof of the structure of TETPE.

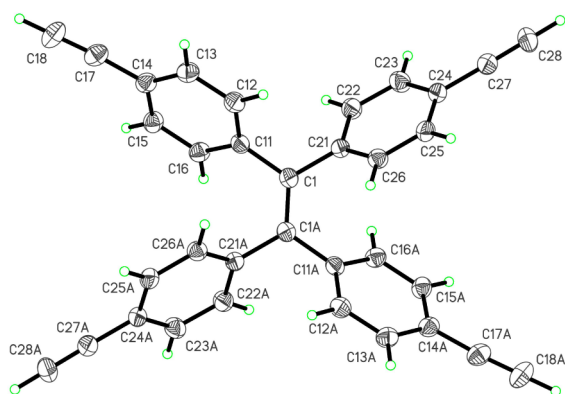


Figure 1. ORTEP drawing of TETPE.

Click Polymerization. The difficulty in the preparation of hyperbranched polymers is the solubility especially for the $A_2 + B_4$ monomer strategy with equal reactive functional groups because the gelation is an ineluctable problem. One of the solutions is to quench the polymerization reaction before the gel points which are unfortunately very difficult to predict and control.¹⁶ Given the efficiency and step-growth mechanism of Cu(I)-catalyzed azide–alkyne click polymerization,⁴ we assumed that if equal concentrations of A_2 (BATPE) and B_4 (TETPE) were used, the azide groups would be consumed rapidly during the polymerization, making the resultant polymer end-capped with the ethynyl groups, and thus no gelation would occur.

We first tried the click polymerization of BATPE and TETPE with the same concentration in the presence of the classical $CuSO_4$ /sodium ascorbate catalyst system in THF/triethylamine mixture with minimal amount of water (Scheme 3 and Scheme S1). Delightfully, no gelation took place even the polymerization was stirred at 60 °C for 12 h under nitrogen and *hb*-CPTA, whose structure is schematically shown in Scheme 3, with M_w of 47 100 was obtained in excellent yield (85.3%) (Table 1, no. 6). It is worth noting that *hb*-CPTA is soluble in most of common used organic solvent, such as THF,

Table 1. Time Courses of the Click Polymerization of BATPE and TETPE^a

no.	<i>t</i> (h)	yield (%)	M_w^b	PDI ^b
1	1.0	49.6	6 500	2.35
2	2.0	75.2	15 900	4.33
3	3.0	81.6	31 100	4.36
4	4.0	83.7	38 900	4.73
5	5.0	84.4	39 500	4.64
6	12.0	85.3	47 100	5.22

^aPolymerizations were carried out in THF/ Et_3N (*v/v* = 10:1) mixture at 60 °C under nitrogen using $CuSO_4$ /sodium ascorbate as catalyst system; [BATPE] = [TETPE] = 0.018 M. ^bRelative value estimated by GPC in THF of the basis of a linear polystyrene calibration, PDI = M_w/M_n .

dichloromethane, chloroform, and *N,N*-dimethylformamide (DMF), but partially soluble in dimethyl sulfoxide (DMSO). Meanwhile, under the same polymerization conditions, gelation was observed within 4 h if equal molar amounts of ethynyl and azide groups were used. These interesting results confirm the practicability of our assumption.

Encouraged by the preliminary results and to make the click polymerization more efficient, we thus systematically investigated its time courses. As can be seen from Table 1, the yields and M_w s of *hb*-CPTA increased rapidly with the reaction time in the first 3 h. Afterward, the increase of both of them slowed down. Thus, 5 h was adopted as the optimal reaction time. It is worth mentioning that the click polymerization possesses excellent repeatability, giving quite similar results under the same polymerization conditions.

Structural Characterization. Thanks to its good solubility, *hb*-CPTA was fully characterized spectroscopically, and satisfactory analysis data corresponding to its expected molecular structure were obtained. The IR spectra of *hb*-CPTA and its monomers are shown in Figure 2. The $\equiv C-H$

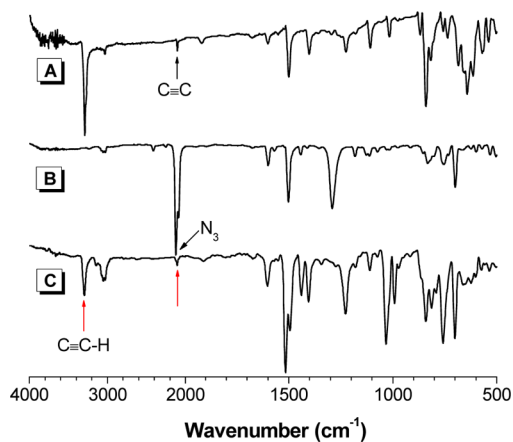
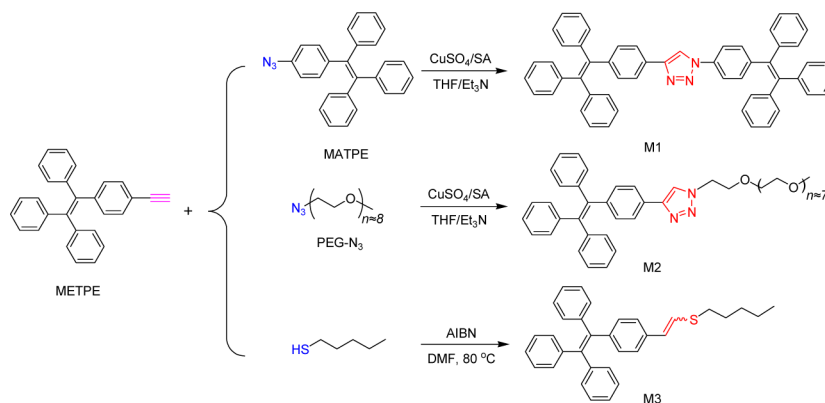


Figure 2. IR spectra of (A) TETPE, (B) BATPE, and (C) *hb*-CPTA.

stretching vibration of TETPE is observed at 3291 cm^{-1} , which becomes moderate after click polymerization, suggesting that a large number of ethynyl groups remained on the periphery of *hb*-CPTA. The azide groups of BATPE exhibit a strong absorption band at 2122 cm^{-1} which almost disappeared after reaction. The weak peak at 2107 cm^{-1} could be attributed to $C\equiv C$ stretching vibration, indicating that the *hb*-CPTA is end-capped with ethynyl groups on its periphery (cf. Scheme 3).

Scheme 4. Synthetic Routes for the Model Compounds (SA = Sodium Ascorbate)



NMR spectroscopy could provide more valuable information for the illustration of the polymer structure. To facilitate the structure characterization of *hb*-CPTA, model compound **M1** was designed and synthesized by click reaction of 1,4-ethynylphenyl)-1,2,2-triphenylethene (named METPE, Scheme S2) and 1-(4-azidophenyl)-1,2,2-triphenylethene (named MATPE, Scheme S3) under the same reaction conditions (Scheme 4).

Figure 3 shows the ^1H NMR spectra of *hb*-CPTA and its monomers (TETPE and BATPE) as well as its model compound (**M1**) in CDCl_3 . The peak (1) of the ethynyl group of TETPE was resonates at δ 3.07 (Figure 3A), whose

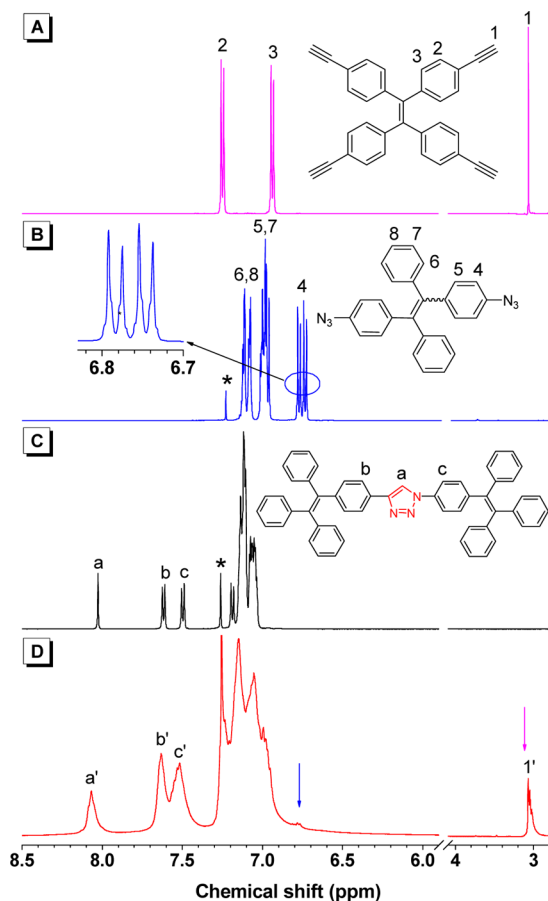


Figure 3. ^1H NMR spectra of (A) TETPE, (B) BATPE, (C) **M1**, and (D) *hb*-CPTA in CDCl_3 . The solvent peaks are marked with asterisks.

intensity keeps relatively strong in the *hb*-CPTA (**1'**, Figure 3D). Meanwhile, the resonance of phenyl proton ortho to the azide groups of BATPE occurs at δ 6.72–6.78 (4), which are well-separated and make it possible to discriminate whether the azides are used up or not after click polymerization (Figure 3B). These resonance peaks are hardly observed in the spectrum of *hb*-CPTA, indicating that azide groups were almost consumed. By comparison with the model compound **M1**, the peak at δ 8.07 (**a'**) in the spectrum of *hb*-CPTA (Figure 3D) could be readily assigned to the proton resonance of the formed 1,4-disubstituted 1,2,3-triazoles (Figure 3C). Because of the electron deficiency and high polarity of triazole unit, the resonance of its adjacent phenyl protons were shifted down filed at δ 7.63 (**b'**) and 7.52 (**c'**) as demonstrated in the spectrum of **M1**.

Furthermore, ^{13}C NMR spectrum of *hb*-CPTA shows strong resonated peaks of ethynyl carbon atoms at δ 83.6 and 77.8 (Figure S3), which means considerable ethynyl groups were remained in the polymer. All the other resonance peaks could be assigned according to the ^{13}C NMR spectrum of **M1**. These results further substantiate the conclusion drawn from the IR analysis.

Determination of Degree of Polymerization (DP).

According to the structural characterization, *hb*-CPTA is composed of TPE and triazole units, and terminal ethynyl groups (Scheme 3), which enable us to evaluate its degree of polymerization (DP) instead of the hardly assessed degree of branching.

Thanks to the rigid conjugated structure of *hb*-CPTA, the possibility of intramolecular cyclization is believed to be extremely low. Thus, to simplify the calculation, we assume that no loop structures were formed during the click polymerization. When carefully investigating the process of click polymerization of BATPE and TETPE, we could find that, except for the first produced triazole that accompanied by two TPE units, one triazole formation corresponds to one TPE unit increase. In other words, the number of TPE is one more than that of triazole in *hb*-CPTA. On the basis of this finding, we could assume that the total number of TPE units in *hb*-CPTA is n , and that stemmed from TETPE is x . Then, the number of triazole units would be $n - 1$, and that of TPE from BATPE is $n - x$.

Accordingly, an equation could be established as follows:

$$\frac{A_t}{A_p} = \frac{n - 1}{16x + 18(n - x)} \quad (1)$$

where A_t and A_p are the integrated areas of proton resonated peaks of the triazole and phenyl units in *hb*-CPTA, respectively.

From the structure characterization, we also concluded that almost all the azides were transformed to the triazole units. Thus, a relationship between the numbers of triazole and the used BATPE could be established:

$$2(n - x) = n - 1 \quad (2)$$

When substituted eq 2 to eq 1, eq 3 could be deduced:

$$\frac{A_t}{A_p} = \frac{n - 1}{17n - 1} \quad (3)$$

As the solvent peak of CDCl_3 could influence the integral of resonance peaks of aromatic protons, the ^1H NMR spectrum of *hb*-CPTA in DCM-d_2 was measured. As shown in Figure S4, the integral ratio of A_t to A_p was obtained as 1/17.10. Introducing this value into eq 3, the DP of *hb*-CPTA is calculated to be 161, from which the number of TPE from TETPE (x) is deduced to be 81 and that from BATPE is 80. Thus, the number-average molecular weight of *hb*-CPTA (M_n) could be derived from eq 4:

$$M_n = xM_{\text{TETPE}} + (n - x)M_{\text{BATPE}} = 67800 \quad (4)$$

where M_{TETPE} and M_{BATPE} are the formula weights of TETPE and BATPE, respectively.

Comparing with the M_n value estimated by GPC, the calculated one is ca. 8 times higher (eq 5) probably because of the globular architecture of the hyperbranched polymer, which normally makes its molecular weight underestimated.¹⁷

$$\frac{M_{n(\text{NMR})}}{M_{n(\text{GPC})}} = \frac{67800}{8500} = 7.98 \quad (5)$$

In addition, based on the calculated results, the theoretical ratio of the number of proton in remained triple bonds to that in triazole could be deduced by eq 6.

$$\frac{N_e}{N_t} = \frac{81 \times 4 - 80 \times 2}{160} = 1.025 \quad (6)$$

where N_e and N_t are the number of remained triple bonds and formed triazole units. The value was thus obtained as 1.025, whereas the experimental ratio from the integrated areas of corresponding peaks in the spectrum of *hb*-CPTA is 0.96 (Figure S4). These two ratios are quite close within the experimental error, verifying that our assumption is reasonable and the DP calculation is reliable.

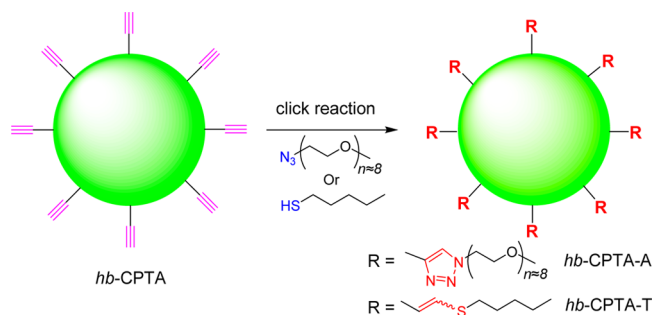
Clickable Modification. Surface modification has been a hot topic in nano- and biomaterial areas because properties of the materials are related to or even dependent on their surface composition.¹⁸ One remarkable feature of hyperbranched polymers is their numerous terminal functional groups on the periphery (surface) which enable to generate versatile functions. For example, attaching of water-soluble segments or biomolecules could make hyperbranched polymers amphiphilic or biocompatible and facilitate their practical applications.

The *hb*-CPTA is end-capped with ethynyl groups according to its structural characterization, which makes it promising to modify by various acetylene reactions, such as azide–alkyne and thiol–yne click reactions.¹⁹ These reactions have been utilized to modify the periphery of hyperbranched polymers with partially or nonconjugated structures.²⁰ However, the

postfunctionalization of hyperbranched conjugated polymers is rare.

Here, we show examples of modification of the periphery of *hb*-CPTA by the azide–alkyne and thiol–yne click reactions (Scheme 5). Thanks to the same catalyst system, monoazide-

Scheme 5. Click Modification of *hb*-CPTA^a



^aThe spheres are symbolized as hyperbranched conjugated polymers.

functionalized poly(ethylene glycol) (PEG- N_3 , Scheme S4) could be added after the click polymerization in one-pot and PEG-functionalized *hb*-CPTA; i.e., *hb*-CPTA-A was produced after an additional 12 h. Interestingly, *hb*-CPTA-A is completely soluble in DMSO but partially in THF because of the attached PEG segments. Furthermore, the M_w of *hb*-CPTA-A (204500) is much higher than that of *hb*-CPTA (89600) with the same measurement conditions using DMF as eluent, indicating that the PEG segments have been successfully grafted on the periphery of *hb*-CPTA.

Since the thiol is a common functional group existing widely in biomolecules, including amino acid (e.g., cysteine), polypeptide (e.g., glutathione), and protein (e.g., bovine serum albumin), etc., the thiol–yne click reaction has special potential in biological fields and thus drawn much attention in recent years.²¹ Attracted by this efficient click reaction,²² we employed pentanethiol as a representative thiol compound to end-cap *hb*-CPTA. The alkyl sulfide-functionalized *hb*-CPTA, i.e., *hb*-CPTA-T, was thus produced after they reacted in DMF at 80 °C for 24 h in the presence of AIBN, a radical initiator (Scheme 5). The solubility of the production is even better than its parent polymer probably due to the alkyl chain attachment. Furthermore, the enhancement of M_w (67400) also suggests the success of the thiol–yne reaction.

Spectroscopic structural characterization of *hb*-CPTA-A and *hb*-CPTA-T could give a clearer vision of the click reactions. As shown in Figure 4, the $\equiv\text{C-H}$ and $\text{C}\equiv\text{C}$ stretching vibrations of *hb*-CPTA disappeared in the IR spectra of *hb*-CPTA-A and *hb*-CPTA-T, indicating that all the remained ethynyl groups have been consumed after click reactions. Meanwhile, the strengthened absorption bands at 2869 and 1108 cm^{-1} for *hb*-CPTA-A and 2925 and 2856 cm^{-1} for *hb*-CPTA-T, which are assigned to the PEG and alkyl chain vibrations, respectively, verified that these segments have been successfully grafted onto the peripheries of *hb*-CPTA.

Similar results could be obtained from the NMR spectra of the polymers. To facilitate the structural characterization of *hb*-CPTA-A and *hb*-CPTA-T, their model compounds **M2** and **M3** were synthesized under the same reaction conditions (Scheme 4). Figure 5 shows the ^1H NMR spectra of *hb*-CPTA-A and its parent polymer *hb*-CPTA as well as its model compound **M2**. The ethynyl protons of *hb*-CPTA resonated at δ 3.07 are hardly

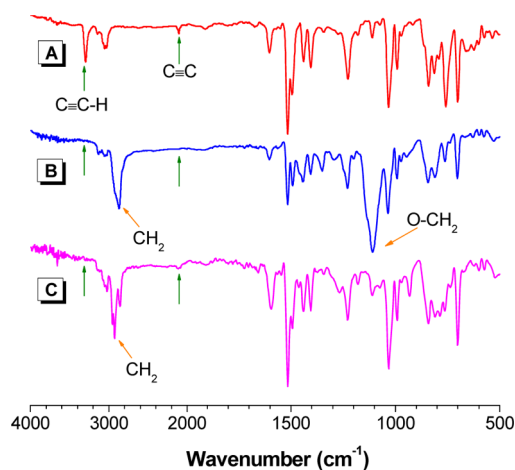


Figure 4. IR spectra of (A) *hb*-CPTA, (B) *hb*-CPTA-A, and (C) *hb*-CPTA-T.

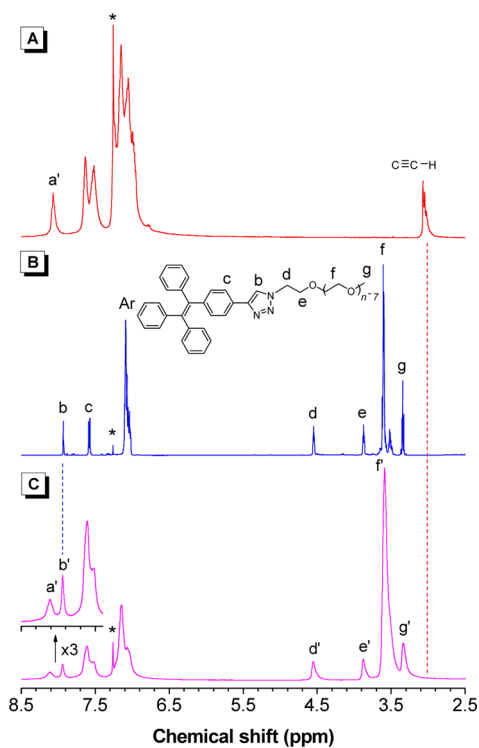


Figure 5. ^1H NMR spectra of (A) *hb*-CPTA, (B) **M2**, and (C) *hb*-CPTA-A in CDCl_3 . The solvent peaks are marked with asterisks.

observed in the spectrum of *hb*-CPTA-A. Meanwhile, new peaks at δ 4.55–3.34, which could be assigned to the PEG segments according to that of **M2**, were emerged. Furthermore, the resonance of protons from the new formed triazole appeared at δ 7.94 (b'), indicating that the ethynyl groups on the periphery of *hb*-CPTA have been completely transformed into triazoles and the efficiency of click reaction reaches 100%.

The ^{13}C NMR spectra (Figure S5) also showed that the ethynyl carbon atoms of *hb*-CPTA resonated at δ 83.6 and 77.8 completely disappeared after reaction, and new peaks emerged at δ 71.9–50.3, which are assigned to the resonance of carbon from PEG segment. These results confirm again that the *hb*-CPTA has been completely modified on its periphery via azide–alkyne click reaction.

The complete consumption of ethynyl groups in the thiol–yne click reaction of *hb*-CPTA and pentanethiol was also proven by the ^1H NMR spectrum. As can be seen from Figure 6, the resonance of ethynyl protons at δ 3.07 could never be

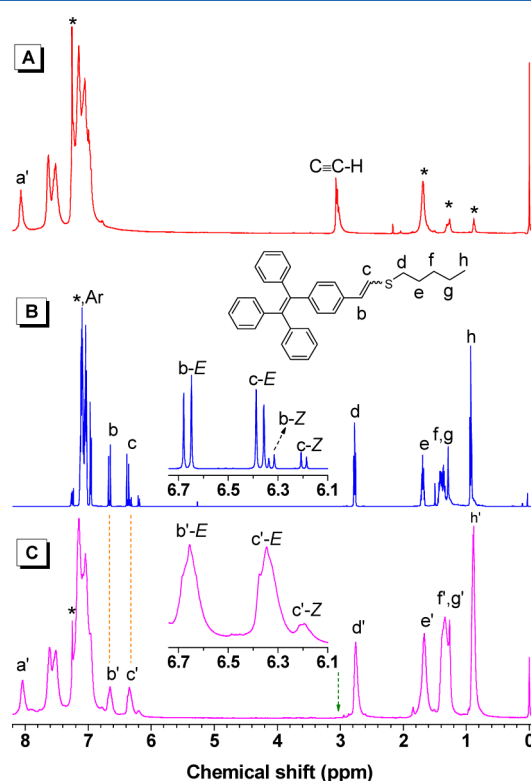


Figure 6. ^1H NMR spectra of (A) *hb*-CPTA, (B) **M3**, and (C) *hb*-CPTA-T in CDCl_3 . The solvent peaks are marked with asterisks.

found in the spectrum of *hb*-CPTA-T. The new peaks at δ 6.66, 6.35, and 6.21 may be stemmed from the vinyl groups,²³ indicating that only one thiol was added to one alkyne. This is an interesting and abnormal result because it was reported that the radical-mediated thiol–yne click reaction allows two thiols to add to one alkyne.^{21,22} In order to prove our assumption, the model reaction was carried out, and only was sole product of **M3** obtained (Scheme 4). Moreover, the increase of the amount of AIBN and pentanethiol did not affect the composition of product. In the ^1H NMR spectrum of **M3**, the integrated area of the vinyl protons is equal to that of the alkyl ones adjacent to the sulfur atom, further substantiating that one thiol was added to one alkyne. The reason could be that the conjugation of the *hb*-CPTA deactivates the vinyl sulfide group and makes further addition quite difficult. It is worth noting that the *E/Z* isomers of generated vinyl units of *hb*-CPTA-T could be identified clearly with the help of the spectrum of **M3**, which was calculated to be 85/15.²³ The ^{13}C NMR of *hb*-CPTA-T (Figure S5) also confirmed that *hb*-CPTA could be efficiently functionalized by the radical-mediated thiol–yne click reaction.

Thermal Stability. The thermal properties of three polytriazoles were evaluated by thermogravimetric analysis (TGA) under nitrogen (Figure 7). The *hb*-CPTA is thermally stable and loses 5% of its weight at temperature (T_d) of 363.3 °C. More importantly, the char yield of *hb*-CPTA was as high as 74.8% at 800 °C, which make it promising carbon sources for graphene, carbon nanotube, etc. Such a high T_d value and char

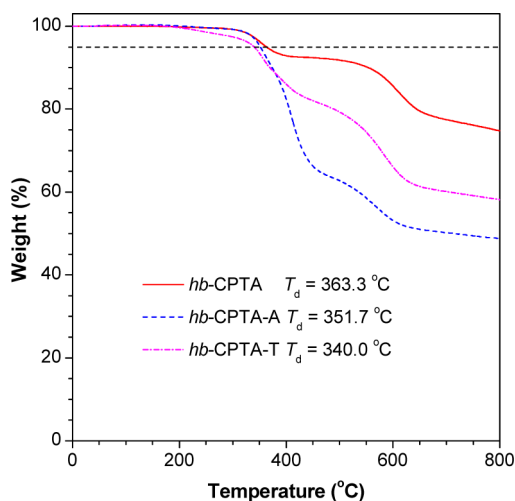


Figure 7. TGA thermograms of *hb-CPTA*, *hb-CPTA-A*, and *hb-CPTA-T* recorded under nitrogen at a heating rate of 20 °C/min.

yield might be attributed to the aromatic conjugated structure of and readily cross-linked triple bonds in *hb-CPTA*.²⁴

The T_d values of *hb-CPTA-A* and *hb-CPTA-T* lowered compared to that of *hb-CPTA*, but they are still higher than 340.0 °C. Their char yields at 800 °C, however, decreased dramatically to 48.8 and 58.2%, respectively, owing to the involved PEG and alkyl chains, which could be pyrolyzed at elevated temperature.

Aggregation-Enhanced Emission. We first measured the absorption spectra of these polytriazoles (Figure S6). *hb-CPTA* exhibits two absorption peaks at 282 and 340 nm. Furthermore, its maximum absorption is bathochromically shifted by 7 nm compared to our previously reported TPE containing partially conjugated hyperbranched polytriazoles due to its fully conjugated feature.^{13a} Meanwhile, the absorption of *hb-CPTA-A* is peaked at 287 and 340 nm, indicating that the formed triazole units exert little influence over the polymer conjugation, whereas the introduction of the vinyl sulfide groups to *hb-CPTA* greatly change the absorption behavior. *hb-CPTA-T* exhibits only one absorption peak at 328 nm, but its spectrum is tailed to a longer wavelength compared to that of *hb-CPTA* and *hb-CPTA-A*.²⁵ The trend is also observed in their photoluminescence (PL) spectra (Figure 8). Thanks to

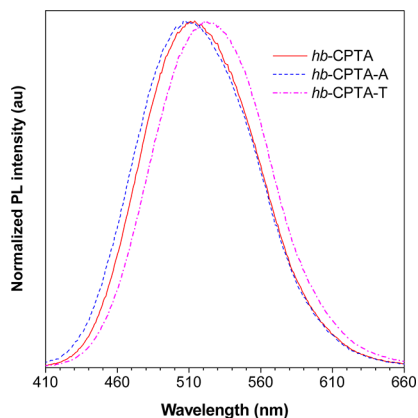


Figure 8. Normalized PL spectra of *hb-CPTA*, *hb-CPTA-A*, and *hb-CPTA-T* in THF. Concentration: 10 $\mu\text{g}/\text{mL}$; excitation wavelength: 340 nm.

the contained TPE units, the THF solutions of *hb-CPTA*, *hb-CPTA-A*, and *hb-CPTA-T* are emissive with maximum peaks at 512, 509, and 524 nm, respectively, which are also redder than that of our previously reported partially conjugated hyperbranched polytriazoles (490 nm).^{13a}

TPE is a typical AIE-active luminogen, whereas the *hb-CPTA*, *hb-CPTA-A*, and *hb-CPTA-T* containing TPE units are AEE-active. The PL spectra of *hb-CPTA* in THF/water mixtures with different water fraction (f_w) are shown in Figure 9A as an example. The UV spectra of *hb-CPTA* in pure THF

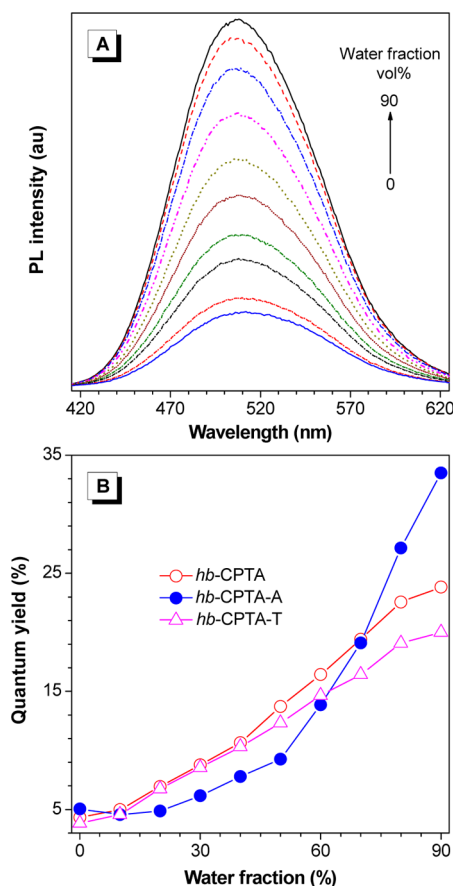


Figure 9. (A) PL spectra of *hb-CPTA* in the THF/water mixtures with different water fraction (f_w). Concentration: 10 $\mu\text{g}/\text{mL}$; excitation wavelength: 340 nm. (B) Changes in the quantum yields (Φ_F) of *hb-CPTA*, *hb-CPTA-A*, and *hb-CPTA-T* with f_w in the THF/water mixtures; Φ_F was estimated using quinine sulfate in 0.05 M H_2SO_4 ($\Phi_F = 54.6\%$) as standard.

and THF/water mixtures show similar profiles, except for the spectral tails in the long wavelength region which are ascribed to the formation of aggregates with high f_w (Figure S7). When excited at 340 nm, the PL intensity starts to increase even at a low f_w of 10% and keeps to rise with gradual addition of water but without a noticeable shift in the emission maximum. The PL spectra of *hb-CPTA-A* and *hb-CPTA-T* in THF/water mixtures share similar processes (Figure S8). Interestingly, due to hydrophilic property of PEG containing *hb-CPTA-A* which is verified by the contact angle measurement (Figure S9), its water solubility is enhanced. Thus, its PL intensity decreases when 10% water is added. Afterward, its emission is slowly intensified until the f_w higher than 50%.

The fluorescence quantum yields (Φ_F) of three polymers in the THF/water mixtures were measured, and their changing

trajectories are shown in Figure 9B. The Φ_F values of *hb*-CPTA, *hb*-CPTA-A, and *hb*-CPTA-T in THF are 4.31, 5.04, and 3.83%, respectively. Thanks to the rigid structures, the Φ_F values of *hb*-CPTA and *hb*-CPTA-T increase linearly with gradual addition of water, whereas the Φ_F value of *hb*-CPTA-A decreases to 4.57% in THF/water mixture with an f_w of 10% and then increases swiftly after $f_w > 50\%$. At an f_w of 90%, the Φ_F values of *hb*-CPTA, *hb*-CPTA-A, and *hb*-CPTA-T are increased to 23.83, 33.48, and 20.01%, respectively. It is worth noting that the absolute Φ_F values of their thin films measured by a calibrated integrated sphere were recorded to be 65.2, 93.5, and 60.2%, respectively, which enable them to find broad application in optoelectronic and biological fields.

Polymer Morphology. Our synthesized AEE-active hyperbranched polymers possess rigid structures; thus, their morphology was examined by the transmission electron microscope (TEM) and fluorescence microscope. The samples were prepared directly by drop-coating the dilute chloroform solutions (0.1 $\mu\text{g}/\text{mL}$) of three polytriazoles onto copper grids. As shown in Figure 10, the particle sizes of *hb*-CPTA are

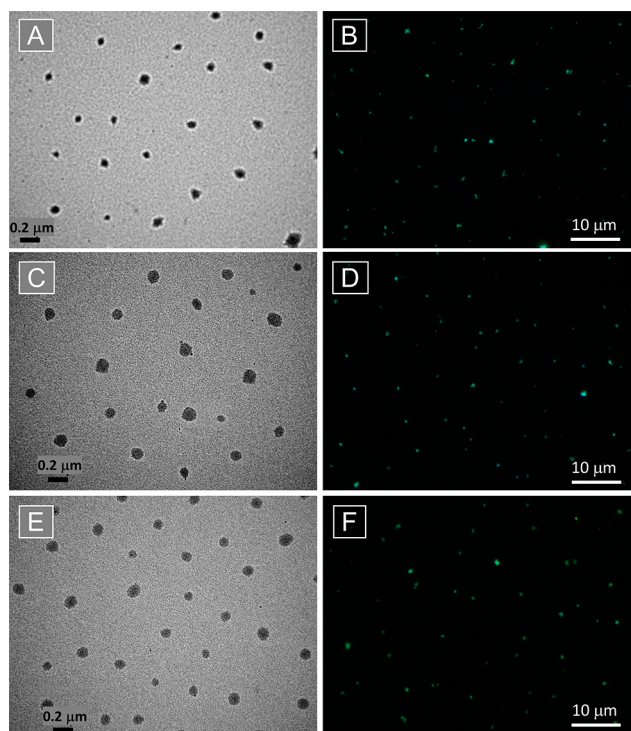


Figure 10. TEM and fluorescent images of (A, B) *hb*-CPTA, (C, D) *hb*-CPTA-A, and (E, F) *hb*-CPTA-T. Samples prepared from their chloroform solution directly, concentration: 0.1 $\mu\text{g}/\text{mL}$. The fluorescent images of the nanoparticles were taken under a fluorescence microscope with a 337 nm excitation.

relatively uniform with diameters around 70–100 nm (Figure 10A). After postclick reactions, the particle sizes increase slightly, to 90–120 nm for *hb*-CPTA-A (Figure 10C) and 80–100 nm for *hb*-CPTA-T (Figure 10E). The increase of the particle sizes of *hb*-CPTA-A and *hb*-CPTA-T stemmed from the attached PEG segments and alkyl chains, respectively.

Their morphology in concentrated solutions (1.0 $\mu\text{g}/\text{mL}$) was tested as well. Though few polymer aggregates were observed, a large number of particles were found to have sizes identical to those from dilute solutions (Figure S10), suggesting that nanoparticles are probably formed from an unimolecule of

the polymers, and the size distribution of the particles comes from the distribution of molecule weights. Thanks to the contained TPE units, the nanoparticles are all emissive. As can be seen from Figure 10, the particles with bluish-green (for *hb*-CPTA and *hb*-CPTA-A in Figures 10B and 10D, respectively) to green (for *hb*-CPTA-T in Figure 10F) emission just like an array of stars in the sky could be clearly observed upon excitation with a UV light. Because of the rigid conjugated structure, the single-molecular fluorescent nanoparticles of the polymers may hold good shape persistence with suitable sizes (around 100 nm) for potential biological applications, such as drug carrier and fluorescence tracing.

CONCLUSION

Soluble ethynyl-capped hyperbranched conjugated polytriazole *hb*-CPTA with high molecular weight was first constructed in high yield via Cu(I)-catalyzed azide–alkyne click polymerization of BATPE and TETPE in equal concentrations. Thanks to the large amount of ethynyl groups on the periphery, *hb*-CPTA could be facilely modified by alkyne-based click reactions. The PEG segment was facilely introduced onto the polymer via azide–alkyne click reaction in one pot, whereas pentanethiol could be efficiently reacted with the remained ethynyl group of *hb*-CPTA through radical-mediated thiol–yne click reaction. Furthermore, one thiol was found to react with only one ethynyl group probably due to the conjugation effect of the polymer. The polytriazoles are thermal stable and *hb*-CPTA shows high char yield of 74.8% at 800 °C. The polymers are emissive in their solutions, and their luminescence intensified in aggregate or solid states, demonstrating a unique AEE feature. Thanks to the rigid structures, the polymers can form unimolecular nanoparticles from their dilute solutions with diameters around 100 nm.

The above results indicate that *hb*-CPTA is a novel clickable fluorescent platform, onto which various functional groups or biomolecules could be grafted efficiently, which will be sure to find wide applications in biological and optoelectronic fields, etc.

EXPERIMENTAL SECTION

Materials. Unless otherwise stated, all the chemicals used in this study were purchased from Acros or Alfa and used as received without further purification. The radical initiator 2,2'-azobis(2-methylpropionitrile) (AIBN) was recrystallized from ethanol before use. Tetrahydrofuran (THF) was distilled from sodium benzophenone ketyl under nitrogen immediately prior to use. Triethylamine (TEA) was distilled and dried over potassium hydroxide. DMF was extra-dry grade.

Instruments. ^1H and ^{13}C NMR spectra were measured on Bruker DMX-500 and Varian NMR-300 spectrometer in CDCl_3 or CD_2Cl_2 using tetramethylsilane (TMS; $\delta = 0$) as internal reference. FT-IR spectra were recorded on a Bruker Vector 22 spectrometer. Melting points (T_m) were measured on a Perkin-Elmer DSC-7 under nitrogen at a heating rate of 10 °C/min. Elemental analysis was performed on a ThermoFinnigan Flash EA1112. MALDI-TOF mass spectra were taken on a GCT Premier CAB048 mass spectrometer. Single-crystal X-ray diffraction intensity data were collected at 173 K on an Xcalibur, Sapphire3, Gemini ultra kappa diffractometer with graphite monochromated Cu $K\alpha$ X-ray radiation. Empirical absorption correction was done by using spherical harmonics, implemented in SCALE3 ABSPACK scaling algorithm. CrysAlisPro, Agilent Technologies, Version 1.171.35.19. The structure solution was measured using XS (Sheldrick 2008), and the structure refinement was conducted using XL (Sheldrick 2008) suite of X-ray programs. Relative number (M_n) and weight-average (M_w) molecular weights and polydispersity indices (PDI) of the polymers were estimated by a Waters PL-GPC-50 gel

permeation chromatography (GPC) system equipped with refractive index (RI) detector, using a set of monodisperse polystyrenes or poly(methyl methacrylate) (PMMA) as calibration standards and THF or DMF as the eluents at a flow rate of 1.0 mL/min. Thermal stabilities were evaluated by measuring thermogravimetric analysis (TGA) thermograms on a Perkin-Elmer TGA 7 under dry nitrogen at a heating rate of 20 °C/min. UV-vis spectra were measured on a Varian VARY 100 Bio UV-vis spectrophotometer. Photoluminescence (PL) spectra were recorded on a Shimadzu RF-5301PC spectrofluorophotometer. Fluorescence quantum yields (Φ_F) were estimated using quinine sulfate in 0.05 M sulfuric acid ($\Phi_F = 54.6\%$) as standard. The absorbance of the solutions was kept around 0.05 to avoid internal filter effect. The Φ_F of spin-coated thin films of the polymers was recorded by a calibrated integrating sphere on a Photon Technology International time-resolved fluorescence spectroscopy.²⁶ Contact angle was measured on DSA100. The morphology of the polymers was checked by a JEOL JEM-1200EX electron microscope (TEM, 80 kV). Fluorescence micrographs were taken on a Zeiss Axiovert 200 microscope equipped with a 100 \times oil immersion objective.

For the AEE measurement, a stock solution of a polymer in THF (0.1 mg/mL) was prepared. Aliquots of this stock solution were transferred into volumetric flasks (10 mL), into which appropriate volumes of THF and water were added dropwise under vigorous stirring to give 10 μ g/mL solutions with different water contents ($f_w = 0$ –90%). UV and PL spectra were measured immediately after the solutions were prepared.

Monomer Preparation. The synthetic routes to TETPE and BATPE are shown in Scheme 1. One of the starting materials of 1,2-bis(4-bromophenyl)-1,2-diphenylethene (**4**) was prepared according to our previously published procedures.^{13a}

4,4'-Bis(trimethylsilyl)benzophenone (2). Into a 500 mL round-bottom flask was added PdCl₂(PPh₃)₂ (561.5 mg, 0.8 mmol), CuI (304.8 mg, 1.6 mmol), PPh₃ (629.5 mg, 2.4 mmol), and 4,4'-dibromobenzophenone (**1**) (6.8 g, 20 mmol), and then a mixture of THF/TEA (1:1 v/v) (200 mL) under nitrogen. After the solution became homogeneous, trimethylsilylacetylene (7.07 mL, 50 mmol) was injected. The solution was allowed to react at 50 °C for 24 h, after which the formed solid was removed by filtration and washed with diethyl ether. The filtrate was concentrated by a rotary evaporator, and the crude product was purified by a silica gel column chromatography using petroleum ether/ethyl acetate mixture (100:1 by volume) as eluent. White solid of **2** was obtained in 89.7% yield (6.720 g). ¹H NMR (300 MHz, CDCl₃) δ (TMS, ppm): 7.69 (d, 4H), 7.54 (d, 4H), 0.27 (s, 18H). ¹³C NMR (75 MHz, CDCl₃) δ (ppm): 195.3, 136.8, 132.0, 129.9, 127.6, 104.1, 98.2, and -0.03.

1,1,2,2-Tetrakis(4-(trimethylsilylethynyl)phenyl)ethene (3). Into a 500 mL two-necked round-bottom flask equipped with a reflux condenser was placed **2** (5.994 g, 16 mmol) and zinc dust (3.137 g, 48 mmol). The flask was evacuated under vacuum and flushed with dry nitrogen three times. After THF (200 mL) was added, the mixture was cooled down to 0 °C, into which TiCl₄ (4.552 g, 2.64 mL, 24 mmol) was added dropwise, then warmed slowly to room temperature, and refluxed overnight. Afterward, the reaction mixture was cooled to room temperature, filtered, and washed with diethyl ether. After most of the solvent was evaporated, the filtrate was poured into 1 M HCl solution (100 mL) and extracted by DCM three times. The organic layer was combined and washed with brine and water and then dried over MgSO₄. After filtration and solvent evaporation, the crude product was purified by a silica gel column chromatography using petroleum ether as eluent. Pale yellow solid of **3** was obtained in 75.4% yield (4.326 g). ¹H NMR (300 MHz, CDCl₃) δ (TMS, ppm): 7.18 (d, 8H), 6.86 (d, 8H), 0.22 (s, 36H). ¹³C NMR (75 MHz, CDCl₃) δ (ppm): 143.2, 140.9, 131.7, 131.3, 121.7, 105.0, 95.0, and 0.07.

1,1,2,2-Tetrakis(4-ethynylphenyl)ethane (TETPE). Into a 500 mL round-bottom flask was placed **3** (4.304 g, 6 mmol) and THF (100 mL). Then KOH (5.376 g, 96 mmol) dissolved in methanol (100 mL) was added. The mixture was stirred at room temperature overnight. After most of the solvent was evaporated, 1 M HCl solution (100 mL) was added and then extracted by DCM three times. The

organic layer was combined and washed with water and brine and then dried over MgSO₄. After filtration and solvent evaporation, the crude product was purified by a silica gel column chromatography using petroleum ether/DCM (100:1 by volume) mixture as eluent. Pale yellow solid of TETPE was obtained in 86.8% yield (2.231 g). T_m : 155.5 °C. IR (KBr) ν (cm⁻¹): 3291 (\equiv C–H stretching), 3032, 2104 (\equiv C stretching), 1600, 1499, 1402, 1225, 1109, 1016, 841, 737, 642. ¹H NMR (500 MHz, CDCl₃) δ (TMS, ppm): 7.24 (d, 8H), 6.93 (d, 8H), 3.07 (s, 4H, HC \equiv). ¹³C NMR (125 MHz, CDCl₃) δ (ppm): 143.3, 140.9, 131.8, 131.3, 120.7, 83.5 (\equiv C–Ar), 77.9 (\equiv C–H). Anal. Calcd for C₃₄H₂₀: C, 95.30; H, 4.70. Found: C, 94.96; H, 4.75. HRMS (MALDI-TOF), m/z calcd C₃₄H₂₀: 428.1565; found: 428.1567.

1,2-Bis(4-azidophenyl)-1,2-diphenylethene (BATPE). Into a 250 mL round-bottom flask was placed 1,2-bis(4-bromophenyl)-1,2-diphenylethene (**4**, 3.677 g, 7.5 mmol). The flask was evacuated under vacuum and flushed with dry nitrogen three times. After THF (80 mL) was added, the solution was cooled down to -78 °C, into which *n*-BuLi (11.25 mL, 18 mmol, 1.6 M in hexane) was added dropwise. The mixture was kept at -78 °C for 2 h and then 3.550 g (18 mmol) of 4-methylbenzenesulfonyl azide (**5**, see the detailed procedure in the Supporting Information) dissolved in 20 mL of THF was added into the flask dropwise. After reacting at -78 °C for 1 h, the mixture was warmed slowly to room temperature and stirred overnight. Afterward, saturated NH₄Cl solution (100 mL) was added to quench the reaction, and THF was evaporated. Then, DCM was added to extract the product three times. The organic layer was combined and washed with water and brine and dried over MgSO₄. After filtration and solvent evaporation, the crude product was purified by a silica gel column chromatography using petroleum ether as eluent. Pale yellow solid of BATPE was obtained in 71.3% yield (2.216 g). T_m : 118.7 °C. IR (KBr) ν (cm⁻¹): 3054, 2122 (N₃ stretching), 1600, 1501, 1291, 1181, 1112, 832, 754, 700. ¹H NMR (500 MHz, CDCl₃) δ (TMS, ppm): 7.12–7.08 (m, 6H), 6.99 (m, 8H), 6.78–6.74 (q, 4H, Ar–H proton ortho to the azido group). ¹³C NMR (125 MHz, CDCl₃) δ (ppm): 143.3, 140.5, 140.2, 138.2–138.1, 132.8, 131.3, 128.0–127.8, 126.8–126.7, 118.5–118.4. Anal. Calcd for C₂₆H₁₈N₆: C, 75.35; H, 4.38; N, 20.28. Found: C, 75.41; H, 4.52; N, 20.37. HRMS (MALDI-TOF), m/z calcd C₂₆H₁₈N₆: 414.1593; found: 414.1593.

Polymer Synthesis. *hb*-CPTA was synthesized via the well-established Cu(I)-catalyzed click polymerization (Scheme S1) of diazide BATPE (**A**₂) and tetrayne TETPE (**B**₄) with the same concentration.

Click Polymerization. Into a 25 mL Schlenk tube was placed equivalent molar amount of BATPE (41.4 mg, 0.1 mmol) and TETPE (42.9 mg, 0.1 mmol). After being evacuated and refilled with dry nitrogen three times, THF (5 mL) and TEA (0.5 mL) were injected into the tube. When the monomers were completely dissolved, freshly prepared aqueous solutions of sodium ascorbate (1 M, 40 μ L, 10 mol % of ethynyl group) and CuSO₄ (1 M, 20 μ L, 5 mol % of ethynyl group) were added subsequently under vigorous stirring. The reaction mixture was stirred at 60 °C under nitrogen for 5 h. After cooled to room temperature, the resultant mixture was diluted with 5 mL of THF and then added dropwise into 300 mL of methanol acidified with 1 mL of a saturated NH₄Cl solution through a cotton filter under stirring. The precipitate was allowed to stand for 1 h and then filtered. The obtained polymer was dissolved again in chloroform and washed with water three times to remove the residual catalysts. The polymer solution was dried over MgSO₄, concentrated, and precipitated into 300 mL of hexane. The precipitate was allowed to stand again for 1 h, collected by filtration, and dried over vacuum at room temperature to a constant weight. Yellow solid of *hb*-CPTA was obtained in 84.4% yield (71.2 mg). M_w 39 500; PDI 4.64 (THF as the eluent). M_w 89 600; PDI 6.67 (DMF as the eluent). IR (KBr) ν (cm⁻¹): 3294 (\equiv C–H stretching), 3052, 2107 (C \equiv C stretching), 1602, 1516, 1495, 1226, 1033, 841, 758, 701. ¹H NMR (500 MHz, CDCl₃) δ (TMS, ppm): 8.07, 7.63, 7.52, 7.23–6.97, 3.07–3.02 (HC \equiv). ¹H NMR (500 MHz, CD₂Cl₂) δ (TMS, ppm): 8.02, 7.53, 7.41, 7.14–6.86, 3.00–2.96 (HC \equiv). ¹³C NMR (125 MHz, CDCl₃) δ (ppm): 148.0, 144.1, 143.8–143.5, 142.7, 141.2, 140.7, 140.5, 135.4, 135.2, 132.7, 132.0–

131.8, 131.3, 128.8, 128.3, 128.0, 127.3, 125.4, 120.7, 120.6, 120.0, 119.8, 117.6, 83.6 ($\equiv\text{C}-\text{Ar}$), 77.8 ($\equiv\text{C}-\text{H}$).

Preparation of Model Compounds. The detailed synthetic procedures for the starting materials of 1-(4-ethynylphenyl)-1,2,2-triphenylethene (METPE) (Scheme S2) and 1-(4-azidophenyl)-1,2,2-triphenylethene (MATPE) (Scheme S3) are given in the Supporting Information.

1,4-Bis(4-(1,2,2-triphenylvinyl)phenyl)-1H-1,2,3-triazole (M1). The main procedures of the preparation of model compound M1 are similar to those of *hb*-CPTA. Equal amounts of METPE (71.3 mg, 0.2 mmol) and MATPE (74.7 mg, 0.2 mmol) were used as reactants. After the reaction mixture was stirred at room temperature under nitrogen overnight, THF and TEA were evaporated and the residue was extracted with DCM. The organic layer was washed sequentially with saturated NH_4Cl solution, water, and brine and then dried over MgSO_4 . After filtration and solvent evaporation, the crude product was purified by a silica gel column using DCM as eluent. White solid of M1 was obtained in 82.4% yield (120.3 mg). IR (KBr) ν (cm^{-1}): 3053, 1601, 1516, 1491, 1231, 1031, 823, 758, 700. ^1H NMR (500 MHz, CDCl_3) δ (TMS, ppm): 8.02 (s, 1H), 7.60 (d, 2H), 7.48 (d, 2H), 7.17 (d, 2H), 7.10 (m, 20H), 7.03 (m, 12H). ^{13}C NMR (125 MHz, CDCl_3) δ (ppm): 148.2, 144.6, 144.0, 143.66, 143.6, 143.5, 143.3, 143.26, 143.15, 142.3, 141.4, 140.4, 139.4, 135.0, 132.7, 131.9, 131.4–131.26, 128.2, 128.0, 127.9, 127.8, 127.76, 127.7, 126.9, 126.8, 126.76, 126.6, 126.57, 126.5, 125.2, 119.7, 117.4.

1-(Poly(ethylene glycol) monomethyl ether)-4-(4-(1,2,2-triphenylvinyl)phenyl)-1H-1,2,3-triazole (M2). The main procedure of the preparation of model compound M2 was synthesized from METPE and PEG-N3 by the similar procedures of M1, during which excess amount of METPE was used to facilitate the purification. The crude product was purified by a silica gel column using ethyl acetate as eluent. Pale yellow solid of M2 was obtained in 74.2% yield (108.5 mg). IR (KBr) ν (cm^{-1}): 3054, 2872, 1598, 1491, 1449, 1355, 1255, 1109, 1035, 853, 759, 702. ^1H NMR (500 MHz, CDCl_3) δ (TMS, ppm): 7.92 (s, 1H), 7.57 (d, 2H), 7.03 (m, 17H), 4.54 (t, 2H), 3.87 (t, 2H), 3.59 (m, 24H), 3.51 (m, 2H), 3.34 (m, 3H). ^{13}C NMR (125 MHz, CDCl_3) δ (ppm): 147.4, 143.6–143.5, 141.2, 140.4, 131.7, 131.3, 131.26, 128.7, 127.7–127.6, 126.5–126.4, 124.9, 120.9, 71.8, 70.5–70.4, 69.5, 59.0, 50.3.

Pentyl(4-(1,2,2-triphenylvinyl)styryl)sulfane (M3). Into a 25 mL Schlenk tube was placed METPE (71.3 mg, 0.2 mmol) and AIBN (4.0 mg, 0.024 mmol, 5 mol % of thiol). After being evacuated and refilled with dry nitrogen three times, DMF (5 mL) was injected into the tube. When the reactants were completely dissolved, pentanethiol (50.0 mg, 59 μL , 0.48 mmol) was added using a syringe. The reaction mixture was then stirred at 80 °C under nitrogen for 24 h. DMF was evaporated, and the crude product was purified by a silica gel column using petroleum ether as eluent. All emissive products were collected and pale yellow solid of M3 was obtained in 85.2% yield (78.5 mg). IR (KBr) ν (cm^{-1}): 3022, 2925, 2857, 1593, 1494, 1270, 1028, 932, 699. ^1H NMR (500 MHz, CDCl_3) δ (TMS, ppm): 7.22 (d, Ar–H proton adjacent to the *Z*-vinylene unit) and 6.92 (d, Ar–H proton adjacent to the *E*-vinylene unit) (2H), 7.10–6.99 (m, 17H), 6.62 (d, =C–H proton from the *E*-vinylene unit) and 6.29 (d, =C–H proton from the *Z*-vinylene unit) (1H), 6.33 (d, =C–H proton from the *E*-vinylene unit) and 6.16 (d, =C–H proton from the *Z*-vinylene unit) (1H), 2.73 (t, 2H), 1.65 (m, 2H), 1.34 (m, 4H), 0.88 (t, 3H). ^{13}C NMR (125 MHz, CDCl_3) δ (ppm): 143.8, 143.7, 142.3, 142.0, 140.9, 140.7, 135.2, 131.7, 131.5, 131.4, 128.0, 127.8–127.7, 127.5, 126.5–126.4, 125.2, 125.0, 124.8, 32.7, 31.1, 29.2, 22.4, 14.1.

Modification via Azide–Alkyne Click Reaction. Monoazide-functionalized poly(ethylene glycol) (PEG- N_3 , Scheme S4 and the detailed synthetic procedures are given in the Supporting Information) was used as the modification agent.

After the polymerization mixture of BATPE and TETPE was stirred at 60 °C for 5 h, a THF solution of PEG- N_3 (1 mL, 150 mg, about 0.4 mmol) was injected into the tube. The resultant mixture was then stirred at 60 °C for an additional 12 h. After cooled to room temperature, the resultant mixture was diluted with 5 mL of THF and then added dropwise into 300 mL of methanol acidified with 1 mL of a

saturated NH_4Cl solution through a cotton filter under stirring. The precipitate was allowed to stand for 1 h and then filtered. The obtained polymer was dissolved again in a proper amount of chloroform, dried over MgSO_4 , and then precipitated into 300 mL of hexane. The precipitate was allowed to stand again for 1 h, collected by filtration, washed with methanol three times, and dried over vacuum at room temperature to a constant weight. Pale yellow solid of *hb*-CPTA-A (115.0 mg) was obtained. M_w 204 500; PDI 6.81 (DMF as the eluent). IR (KBr) ν (cm^{-1}): 3053, 2869, 1605, 1515, 1492, 1350, 1228, 1108, 1035, 843, 762, 703. ^1H NMR (500 MHz, CDCl_3) δ (TMS, ppm): 8.11, 7.94, 7.61–7.52, 7.15–7.04, 4.55, 3.88, 3.59, 3.34. ^{13}C NMR (125 MHz, CDCl_3) δ (ppm): 148.1, 147.4, 144.0–143.2, 142.7, 140.7, 135.3, 132.6, 132.1–131.9, 131.3, 128.3, 128.0, 127.3, 125.6–125.2, 121.1, 119.7, 117.6, 71.9, 70.5, 69.6, 59.0, 50.3.

Modification via Thiol–Yne Click Reaction. Pentanethiol was adopted as a representative thiol compound to modify *hb*-CPTA.

Into a 25 mL Schlenk tube were placed *hb*-CPTA (50.0 mg) and AIBN (3.3 mg, 0.02 mmol). After being evacuated and refilled with dry nitrogen three times, DMF (5 mL) was injected into the tube. When the polymer was completely dissolved, pentanethiol (41.7 mg, 49 μL , 0.4 mmol) was added via a syringe. The reaction mixture was stirred at 80 °C under nitrogen for 24 h. After cooled to room temperature, the resultant mixture was diluted with 5 mL of THF and then added dropwise into 300 mL of methanol through a cotton filter under stirring. The precipitate was allowed to stand for 1 h and then filtered. The obtained polymer was dissolved again in a proper amount of chloroform, dried over MgSO_4 , and precipitated into 300 mL of hexane. The precipitate was allowed to stand again for 1 h, collected by filtration, and dried over vacuum at room temperature to a constant weight. Orange-yellow solid of *hb*-CPTA-T (65.0 mg) was obtained. M_w 67 400; PDI 5.90 (THF as the eluent). IR (KBr) ν (cm^{-1}): 3022, 2925, 2856, 1593, 1516, 1493, 1228, 1032, 841, 702. ^1H NMR (500 MHz, CDCl_3) δ (TMS, ppm): 8.05, 7.62, 7.52, 7.15–6.97, 6.66, 6.35, 6.21, 2.76, 1.67, 1.35, 0.89. ^{13}C NMR (125 MHz, CDCl_3) δ (ppm): 148.2, 144.0, 142.7, 142.1, 141.9, 140.7, 135.5, 135.4, 135.3, 132.8–132.6, 132.1, 131.8, 131.3, 128.3, 128.1, 128.0, 127.3, 126.2, 125.6–125.2, 124.9, 120.0, 119.7, 117.6–117.5, 32.6, 31.0, 29.2, 22.3, 14.0.

■ ASSOCIATED CONTENT

📄 Supporting Information

Scheme of click polymerization; detailed procedures and characterization data for PEG- N_3 , METPE, and MATPE; crystal data and structure refinement for TETPE; HRMS spectra of TETPE and BATPE; ^1H NMR spectra of *hb*-CPTA in $\text{DCM}-d_2$; ^{13}C NMR spectra of monomers, model compounds, and polymers; normalized UV spectra of the polymers in THF; UV and PL spectra for the polymers in THF/water mixtures; contact angle results; TEM images of samples made from chloroform solution with concentration of 1.0 $\mu\text{g}/\text{mL}$. This material is available free of charge via the Internet at <http://pubs.acs.org>.

■ AUTHOR INFORMATION

✉ Corresponding Author

*E-mail: qinaj@zju.edu.cn (A.Q.); sunjz@zju.edu.cn (J.Z.S.); tangbenz@ust.hk (B.Z.T.).

Notes

The authors declare no competing financial interest.

■ ACKNOWLEDGMENTS

We thank Prof. Yuguang Ma and Dr. Ping Lu for the measurement of the solid-state quantum yields. This work was partly supported by the Natural National Science Foundation of China (21174120, 21074113, 20974028, and 20974098), the Ministry of Science and Technology of China (2009CB623605), the Research Grants Council of Hong

Kong (603509, HKUST2/CRF/10, and N_HKUST620/11), and the University Grants Committee of Hong Kong (AoE/P-03/08). B.Z.T. thanks the support from Cao Guangbiao Foundation of Zhejiang University.

REFERENCES

- (1) (a) Rostovtsev, V. V.; Green, L. G.; Fokin, V. V.; Sharpless, K. B. *Angew. Chem., Int. Ed.* **2002**, *41*, 2596. (b) Tornøe, C. W.; Christensen, C.; Meldal, M. *J. Org. Chem.* **2002**, *67*, 3057. (c) Kolb, H. C.; Finn, M. G.; Sharpless, K. B. *Angew. Chem., Int. Ed.* **2001**, *40*, 2004.
- (2) For recent reviews, see: (a) Chu, C.; Liu, R. *Chem. Soc. Rev.* **2011**, *40*, 2177. (b) Franc, G.; Kakkar, A. K. *Chem. Soc. Rev.* **2010**, *39*, 1536. (c) Hein, J. E.; Fokin, V. V. *Chem. Soc. Rev.* **2010**, *39*, 1302. (d) Mamidala, S. K.; Finn, M. G. *Chem. Soc. Rev.* **2010**, *39*, 1252. (e) Holub, J. M.; Kirshenbaum, K. *Chem. Soc. Rev.* **2010**, *39*, 1325. (f) Lodge, T. P. *Macromolecules* **2009**, *42*, 3827. (g) Carlmark, A.; Hawker, C.; Hult, A.; Malkoch, M. *Chem. Soc. Rev.* **2009**, *38*, 352. (h) Amblard, F.; Cho, J. H.; Schinazi, R. F. *Chem. Rev.* **2009**, *109*, 4207. (i) Meldal, M.; Tornøe, C. W. *Chem. Rev.* **2008**, *108*, 2952. (j) Lutz, J. F.; Börner, H. G. *Prog. Polym. Sci.* **2008**, *33*, 1. (k) Angell, Y. L.; Burgess, K. *Chem. Soc. Rev.* **2007**, *36*, 1674. (l) Moses, J. E.; Moorhouse, A. D. *Chem. Soc. Rev.* **2007**, *36*, 1249. (m) Dondoni, A. *Chem.—Asian J.* **2007**, *2*, 700. (n) Voit, B. *New J. Chem.* **2007**, *31*, 1139.
- (3) (a) Fu, R.; Fu, G.-D. *Polym. Chem* **2011**, *2*, 465. (b) Golas, P. L.; Matyjaszewski, K. *Chem. Soc. Rev.* **2010**, *39*, 1338. (c) Pu, K. Y.; Shi, J. B.; Wang, L.; Cai, L.; Wang, G.; Liu, B. *Macromolecules* **2010**, *43*, 9690. (d) Chen, L.; Shi, N.; Qian, Y.; Xie, L.; Fang, Q.; Huang, W. *Prog. Chem.* **2010**, *22*, 406. (e) Michinobu, T. *Pure Appl. Chem.* **2010**, *82*, 1001. (f) Binder, W. H.; Sachsenhofer, R. *Macromol. Rapid Commun.* **2008**, *29*, 952. (g) Lecomte, P.; Riva, R.; Jécôme, C.; Jécôme, R. *Macromol. Rapid Commun.* **2008**, *29*, 982. (h) Fournier, D.; Hoogenboom, R.; Schubert, U. S. *Chem. Soc. Rev.* **2007**, *36*, 1369. (i) Yagci, Y.; Tasdelen, M. A. *Prog. Polym. Sci.* **2006**, *31*, 1133. (j) Goodall, G. W.; Hayes, W. *Chem. Soc. Rev.* **2006**, *35*, 280. (k) Hawker, C. J.; Wooley, K. L. *Science* **2005**, *309*, 1200. (l) Helms, B.; Mynar, J. L.; Hawker, C. J.; Fréchet, J. M. J. *J. Am. Chem. Soc.* **2004**, *126*, 15020.
- (4) (a) Qin, A. J.; Lam, J. W. Y.; Tang, B. Z. *Chem. Soc. Rev.* **2010**, *39*, 2522. (b) Qin, A. J.; Lam, J. W. Y.; Tang, B. Z. *Macromolecules* **2010**, *43*, 8693. (c) Sumerlin, B. S.; Vogt, A. P. *Macromolecules* **2010**, *43*, 1. (d) Lo, C. N.; Hsu, C. S. *J. Polym. Sci., Part A: Polym. Chem.* **2011**, *49*, 3355. (e) Park, J. S.; Kim, Y. H.; Song, M.; Kim, C. H.; Karim, M. A.; Lee, J. W.; Gal, Y. S.; Kumar, P.; Kang, S. W.; Jin, S. H. *Macromol. Chem. Phys.* **2011**, *211*, 2464. (f) Schwartz, E.; Breitenkamp, K.; Fokin, V. V. *Macromolecules* **2011**, *44*, 4735. (g) Li, Z. A.; Wu, W.; Qiu, G.; Yu, G.; Liu, Y.; Ye, C.; Qin, J.; Li, Z. *J. Polym. Sci., Part A: Polym. Chem.* **2010**, *49*, 1977. (h) Qin, A.; Lam, J. W. Y.; Jim, C. K. W.; Zhang, L.; Yan, J.; Häußler, M.; Liu, J.; Dong, Y.; Liang, D.; Chen, E.; Jia, G.; Tang, B. Z. *Macromolecules* **2008**, *41*, 3808. (i) Li, D. Z.; Wang, X.; Jia, Y. T.; Wang, A. Q.; Wu, Y. G. *Chin. J. Chem.* **2012**, *30*, 861. (j) Li, H.; Sun, J. Z.; Qin, A.; Tang, B. Z. *Chin. J. Polym. Sci.* **2012**, *30*, 1.
- (5) (a) Wu, P.; Feldman, A. K.; Nugent, A. K.; Hawker, C. J.; Scheel, A.; Voit, B.; Pyun, J.; Fréchet, J. M. J.; Sharpless, K. B.; Fokin, V. V. *Angew. Chem., Int. Ed.* **2004**, *43*, 3928. (b) Li, Z.; Wu, W.; Li, Q.; Yu, G.; Xiao, L.; Liu, Y.; Ye, C.; Qin, J.; Li, Z. *Angew. Chem., Int. Ed.* **2010**, *49*, 2763.
- (6) (a) Voit, B. I.; Lederer, A. *Chem. Rev.* **2009**, *109*, 5924. (b) Liu, J.; Lam, J. W. Y.; Tang, B. Z. *Chem. Rev.* **2009**, *109*, 5799. (c) Häußler, M.; Tang, B. Z. *Adv. Polym. Sci.* **2007**, *209*, 1. (d) Khandare, J.; Calderon, M.; Dagia, N. M.; Haag, R. *Chem. Soc. Rev.* **2012**, *41*, 2824. (e) Yates, C. R.; Hayes, W. *Eur. Polym. J.* **2004**, *40*, 1257. (f) Gao, H.; Yorifuji, D.; Wakita, J.; Jiang, Z.; Ando, S. *Polymer* **2010**, *51*, 3173. (g) Perumal, O.; Khandare, J.; Kolhe, P.; Kannan, S.; Lieh-Lai, M.; Kannan, R. M. *Bioconjugate Chem.* **2009**, *20*, 842. (h) Häußler, M.; Qin, A.; Tang, B. Z. *Polymer* **2007**, *48*, 6181. (i) Gao, C.; Yan, D. *Prog. Polym. Sci.* **2004**, *29*, 183.
- (7) (a) Hu, Y.; Chen, L.; Guo, Z.; Nagai, A.; Jiang, D. *J. Am. Chem. Soc.* **2011**, *133*, 17622. (b) Wu, W.; Ye, S.; Huang, L.; Xiao, L.; Fu, Y.; Huang, Q.; Yu, G.; Liu, Y.; Qin, J.; Li, Q.; Li, Z. *J. Mater. Chem.* **2012**, *22*, 6374. (c) Liu, J.; Zhong, Y.; Lam, J. W. Y.; Lu, P.; Hong, Y.; Yu, Y.; Yue, Y.; Faisal, M.; Sung, H. H. Y.; Williams, I. D.; Wong, K. S.; Tang, B. Z. *Macromolecules* **2010**, *43*, 4921. (d) Hu, R.; Lam, J. W. Y.; Liu, J.; Sung, H. H. Y.; Williams, I. D.; Yue, Z.; Wong, K. S.; Yuen, M. M. F.; Tang, B. Z. *Polym. Chem.* **2012**, *3*, 1481. (e) Yuan, W.; Hu, R.; Lam, J. W. Y.; Xie, N.; Jim, C. K. W.; Tang, B. Z. *Chem.—Eur. J.* **2012**, *18*, 2847. (f) Shu, W.; Guan, C.; Guo, W.; Wang, C.; Shen, Y. *J. Mater. Chem.* **2012**, *22*, 3075. (g) Wu, W.; Ye, S.; Yu, G.; Liu, Y.; Qin, J.; Li, Z. *Macromol. Rapid Commun.* **2012**, *33*, 164.
- (8) (a) Birks, J. B. *Photophysics of Aromatic Molecules*; Wiley: London, 1970. (b) Mullen, K.; Scherf, U. *Organic Light-Emitting Devices: Synthesis, Properties and Applications*; Wiley: Weinheim, 2006. (c) Grimsdale, A. C.; Chan, K. L.; Martin, R. E.; Jokisz, P. G.; Holmes, A. B. *Chem. Rev.* **2009**, *109*, 897. (d) Wang, M.; Zhang, G.; Zhang, D.; Zhu, D.; Tang, B. Z. *J. Mater. Chem.* **2010**, *20*, 1858. (e) Xia, J.; Wu, Y.-M.; Zhang, Y.-L.; Tong, B.; Shi, J.-B.; Zhi, J.-G.; Dong, Y.-P. *Imaging Sci. Photochem.* **2012**, *30*, 9.
- (9) (a) Wang, J.; Mei, J.; Qin, A.; Sun, J. Z.; Tang, B. Z. *Sci. China Chem.* **2010**, *53*, 2409. (b) Zheng, R. H.; Häußler, M.; Dong, H. C.; Lam, J. W. Y.; Tang, B. Z. *Macromolecules* **2006**, *39*, 7973. (c) Pu, K.-Y.; Li, K.; Shi, J.; Liu, B. *Chem. Mater.* **2009**, *21*, 3816.
- (10) (a) Luo, J.; Xie, Z.; Lam, J. W. Y.; Cheng, L.; Chen, H.; Qiu, C.; Kwok, H. S.; Zhan, X.; Liu, Y.; Zhu, D.; Tang, B. Z. *Chem. Commun.* **2001**, 1740. (b) Hong, Y.; Lam, J. W. Y.; Tang, B. Z. *Chem. Commun.* **2009**, 4332. (c) Hong, Y.; Lam, J. W. Y.; Tang, B. Z. *Chem. Soc. Rev.* **2011**, *40*, 5361. (d) Zhao, Z.; Wang, Z.; Lu, P.; Chan, C. Y. K.; Liu, D.; Lam, J. W. Y.; Sung, H. H. Y.; Williams, I. D.; Ma, Y.; Tang, B. Z. *Angew. Chem., Int. Ed.* **2009**, *48*, 7608. (e) Li, Z.; Dong, Y. Q.; Lam, J. W. Y.; Sun, J.; Qin, A.; Häußler, M.; Dong, Y. P.; Sung, H. H. Y.; Williams, I. D.; Kwok, H. S.; Tang, B. Z. *Adv. Funct. Mater.* **2009**, *19*, 905.
- (11) (a) Wang, J.; Mei, J.; Hu, R.; Sun, J. Z.; Qin, A.; Tang, B. Z. *J. Am. Chem. Soc.* **2012**, *134*, 9956. (b) Tseng, N.-W.; Liu, J.; Ng, J. C. Y.; Lam, J. W. Y.; Sung, H. H. Y.; Williams, I. D.; Tang, B. Z. *Chem. Sci.* **2012**, *3*, 493. (c) Pu, K. Y.; Liu, B. *Adv. Funct. Mater.* **2009**, *19*, 277. (d) Peng, Q.; Yi, Y.; Shuai, Z.; Shao, J. J. *Am. Chem. Soc.* **2007**, *129*, 9333. (e) Yeh, H. C.; Yeh, S. J.; Chen, C. T. *Chem. Commun.* **2003**, 2632. (f) Qin, A.; Lam, J. W. Y.; Mahtab, F.; Jim, C. K. W.; Tang, L.; Sun, J. Z.; Sung, H. H. Y.; Williams, I. D.; Tang, B. Z. *Appl. Phys. Lett.* **2009**, *94*, 253308. (g) Chen, J.; Law, C. C. W.; Lam, J. W. Y.; Dong, Y. P.; Lo, S. M. F.; Williams, I. D.; Zhu, D.; Tang, B. Z. *Chem. Mater.* **2003**, *15*, 1535.
- (12) (a) Lu, P.; Lam, J. W. Y.; Liu, J.; Jim, C. K. W.; Yuan, W.; Xie, N.; Zhong, Y.; Hu, Q.; Wong, K. S.; Cheuk, K. K. L.; Tang, B. Z. *Macromol. Rapid Commun.* **2010**, *31*, 834. (b) Wu, J.; Liu, W.; Ge, J.; Zhang, H.; Wang, P. *Chem. Soc. Rev.* **2011**, *40*, 3483. (c) Kim, H. N.; Guo, Z.; Zhu, W.; Yoon, J.; Tian, H. *Chem. Soc. Rev.* **2011**, *40*, 79. (d) Chi, Z.; Zhang, X.; Xu, B.; Zhou, X.; Ma, C.; Zhang, Y.; Liu, S.; Xu, J. *J. Chem. Soc. Rev.* **2012**, *41*, 3878.
- (13) (a) Wang, J.; Mei, J.; Yuan, W.; Lu, P.; Qin, A.; Sun, J.; Ma, Y.; Tang, B. Z. *J. Mater. Chem.* **2011**, *21*, 4056. (b) Qin, A.; Tang, L.; Lam, J. W. Y.; Jim, C. K.; Zhao, H.; Sun, J.; Tang, B. Z. *Macromolecules* **2009**, *42*, 1421. (c) Qin, A. J.; Tang, L.; Lam, J. W. Y.; Jim, C. K. W.; Yu, Y.; Zhao, H.; Sun, J. Z.; Tang, B. Z. *Adv. Funct. Mater.* **2009**, *19*, 1891. (d) Li, H.; Wang, J.; Sun, J. Z.; Hu, R.; Qin, A.; Tang, B. Z. *Polym. Chem.* **2012**, *3*, 1075. (e) Li, H. K.; Mei, J.; Wang, J.; Zhang, S.; Zhao, Q.; Wei, Q.; Qin, A. J.; Sun, J. Z.; Tang, B. Z. *Sci. China Chem.* **2011**, *54*, 611. (f) Qin, A.; Zhang, Y.; Han, N.; Mei, J.; Sun, J.; Fan, W.; Tang, B. Z. *Sci. China Chem.* **2012**, *55*, 772.
- (14) (a) Thomas, S. W.; Joly, G. D.; Swager, T. M. *Chem. Rev.* **2007**, *107*, 1339. (b) Sirringhaus, H.; Tessler, N.; Friend, R. H. *Science* **1998**, *280*, 1741. (c) Chen, C.-P.; Chan, S.-H.; Chao, T.-C.; Ting, C.; Ko, B.-T. *J. Am. Chem. Soc.* **2008**, *130*, 12828. (d) Katz, H. E.; Bao, Z.; Gilat, S. L. *Acc. Chem. Rev.* **2001**, *34*, 359. (e) Jager, E. W. H.; Smela, E.; Inganäs, O. *Science* **2000**, *290*, 1540. (f) Xie, Z.; Yoon, S.-J.; Park, S. Y. *Adv. Funct. Mater.* **2010**, *20*, 1638.

- (15) Qin, A. J.; Lam, J. W. Y.; Tang, B. Z. *Prog. Polym. Sci.* **2012**, *37*, 182.
- (16) (a) Kricheldorf, H. R. *Acc. Chem. Res.* **2009**, *42*, 981. (b) Gao, H. F.; Matyjaszewski, K. *Prog. Polym. Sci.* **2009**, *34*, 317. (c) Unal, S.; Long, T. E. *Macromolecules* **2006**, *39*, 2788. (d) Unal, S.; Oguz, C.; Yilgor, E.; Gallivan, M.; Long, T. E.; Yilgor, I. *Polymer* **2005**, *46*, 4533. (e) Yang, X.; Wang, L.; He, X. *J. Polym. Sci., Part A: Polym. Chem.* **2010**, *48*, 5072.
- (17) Qin, A.; Lam, J. W. Y.; Dong, H.; Lu, W.; Jim, C. K. W.; Dong, Y. Q.; Häußler, M.; Sung, H. H. Y.; Williams, I. D.; Wong, G. K. L.; Tang, B. Z. *Macromolecules* **2007**, *40*, 4879.
- (18) (a) Meyers, S. R.; Grinstaff, M. W. *Chem. Rev.* **2012**, *112*, 1615. (b) Neoh, K. G.; Kang, E. T. *Soft Matter* **2012**, *8*, 2057. (c) Chalker, J. M.; Bernardes, G. J. L.; Davis, B. G. *Acc. Chem. Res.* **2011**, *44*, 730. (d) Ye, Q.; Zhou, F.; Liu, W. *Chem. Soc. Rev.* **2011**, *40*, 4244.
- (19) (a) Nebhani, L.; Barner-Kovollik, C. *Adv. Mater.* **2009**, *21*, 3442. (b) Krovi, S. A.; Smith, D.; Nguyen, S. T. *Chem. Commun.* **2010**, *46*, 5277. (c) Rousseau, G.; Fensterbank, H.; Bacsko, K.; Cano, M.; Allard, E.; Larpent, C. *Macromolecules* **2012**, *45*, 3513. (d) Manova, R.; van Beek, T. A.; Zuilhof, H. *Angew. Chem., Int. Ed.* **2011**, *50*, 5428. (e) Angell, Y. L.; Burgess, K. *Chem. Soc. Rev.* **2007**, *36*, 1674. (f) Li, Z.; Wu, W.; Hu, P.; Wu, X.; Yu, G.; Liu, Y.; Ye, C.; Li, Z.; Qin, J. *Dyes Pigm.* **2009**, *81*, 264.
- (20) (a) Han, J.; Li, S.; Tang, A.; Gao, C. *Macromolecules* **2012**, *45*, 4966. (b) Saha, A.; Ramakrishnan, S. *Macromolecules* **2009**, *42*, 4028. (c) Roy, R. K.; Ramakrishnan, S. *Macromolecules* **2011**, *44*, 8398. (d) Li, Z. A.; Yu, G.; Hu, P.; Ye, C.; Liu, Y. Q.; Qin, J. G.; Li, Z. *Macromolecules* **2009**, *42*, 1589.
- (21) (a) Aimetti, A. A.; Feaver, K. R.; Anseth, K. S. *Chem. Commun.* **2010**, *46*, 5781. (b) Minozzi, M.; Monesi, A.; Nanni, D.; Spagnolo, P.; Marchetti, N.; Massi, A. *J. Org. Chem.* **2011**, *76*, 450. (c) Wu, J.-T.; Huang, C.-H.; Liang, W.-C.; Wu, Y.-L.; Yu, J.; Chen, H.-Y. *Macromol. Rapid Commun.* **2012**, *33*, 922. (d) Cai, T.; Neoh, K. G.; Kang, E. T. *Macromolecules* **2011**, *44*, 4258.
- (22) (a) Hoogenboom, R. *Angew. Chem., Int. Ed.* **2010**, *49*, 3415. (b) Hoyle, C. E.; Lowe, A. B.; Bowman, C. N. *Chem. Soc. Rev.* **2010**, *39*, 1355. (c) Chan, J. W.; Hoyle, C. E.; Lowe, A. B. *J. Am. Chem. Soc.* **2009**, *131*, 5751. (d) Fairbanks, B. D.; Scott, T. F.; Kloxin, C. J.; Anseth, K. S.; Bowman, C. N. *Macromolecules* **2009**, *42*, 211. (e) Ren, N.; Huang, X.; Huang, X.; Qian, Y.; Wang, C.; Xu, Z. *J. Polym. Sci., Part A: Polym. Chem.* **2012**, *50*, 3149.
- (23) (a) Liu, J.; Lam, J. W. Y.; Jim, C. K. W.; Ng, J. C. Y.; Shi, J.; Su, H.; Yeung, K. F.; Hong, Y.; Faisal, M.; Yu, Y.; Wong, K. S.; Tang, B. Z. *Macromolecules* **2011**, *44*, 68. (b) Jim, C. K. W.; Qin, A.; Lam, J. W. Y.; Faisal, M.; Yu, Y.; Tang, B. Z. *Adv. Funct. Mater.* **2010**, *20*, 1319.
- (24) (a) Hergenrother, P. M. In *Concise Encyclopedia of Polymer Science and Engineering*; Kroschwitz, J. I., Ed.; Wiley: New York, 1990. (b) Shen, J. Y.; Lee, C. Y.; Huang, T. H.; Lin, J. T.; Tao, Y. T.; Chien, C. H.; Tsai, C. J. *Mater. Chem.* **2005**, *15*, 2455.
- (25) (a) Frank, B. B.; Laporta, P. R.; Breiten, B.; Kuzyk, M. C.; Jarowski, P. D.; Schweizer, W. B.; Seiler, P.; Biaggio, I.; Boudon, C.; Gisselbrecht, J.-P.; Diederich, F. *Eur. J. Org. Chem.* **2011**, 4307. (b) Egbe, D. A. M.; Carbonnier, B.; Birckner, E.; Grummt, U.-W. *Prog. Polym. Sci.* **2009**, *34*, 1023.
- (26) Kawamura, Y.; Sasabe, H.; Adachi, C. *Jpn. J. Appl. Phys.* **2004**, *43*, 7729.